

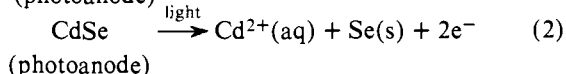
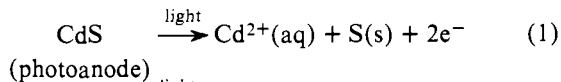
Optical to Electrical Energy Conversion. Characterization of Cadmium Sulfide and Cadmium Selenide Based Photoelectrochemical Cells

Arthur B. Ellis,¹ Steven W. Kaiser, and Mark S. Wrighton*²

Contribution from the Department of Chemistry, Massachusetts Institute of Technology, Cambridge, Massachusetts 02139. Received April 1, 1976

Abstract: Studies are reported on CdS and CdSe based photoelectrochemical cells using aqueous sulfide or polysulfide electrolytes. The key finding is that both n-type CdS and CdSe are stabilized to photoanodic dissolution (irreversible decomposition). The reaction occurring at the photoanode (CdS or CdSe) is the oxidation of the sulfide or polysulfide. But a polysulfide electrolyte undergoes no net chemical change, since the cathode reaction is the reduction of some polysulfide species. The onset of photoresponse for CdSe and CdS based cells is near the band gap of the photoelectrode corresponding to ~ 750 nm for CdSe and ~ 520 nm for CdS. Open circuit photopotentials of up to 0.8 V for CdS and up to 0.65 V for CdSe have been observed in the polysulfide electrolyte. Overall optical to electrical energy conversion of $\sim 7\%$ for CdS at 500 nm and $\sim 9\%$ for CdSe at 632.8 nm with an output voltage of ~ 0.3 V can be realized at low light intensity. Estimated solar energy conversion efficiency for CdSe is $\sim 2\%$.

Recently, we communicated³ preliminary results showing that both n-type CdS and CdSe based *photoelectrochemical cells* can be used as devices for the sustained conversion of low energy visible light to electricity. Our discovery³ was that either sulfide or polysulfides in aqueous solution "quench" the photoanodic dissolution of CdS⁴⁻⁶ and CdSe,^{7,8} reactions 1 and 2, respectively.



We found that the sulfide or polysulfide in the electrolyte is oxidized at the photoelectrode at the expense of either the S^{2-} of the CdS lattice or the Se^{2-} of the CdSe lattice. Previous workers have shown that $\text{Fe}(\text{CN})_6^{4-}$, I^- , and quinones can be oxidized⁷⁻¹⁰ at the CdS or CdSe photoelectrodes. However, the oxidation of these was not shown to completely quench photoanodic dissolution of the CdS and CdSe. It is interesting to note that it was suggested in 1966¹¹ that added sulfide might quench the photoanodic dissolution of CdS.

Stabilization of n-type semiconductors to photoanodic dissolution is very important, since the photoanodic dissolution of CdS and CdSe is a typical,¹² rather than exceptional, result. Stability of the photoelectrode is a key requirement for an optical energy conversion device. It has been known since early in the 19th century¹³ that irradiation of an electrode in an electrochemical cell can result in a photocurrent, and therefore one can, in principle, use the device to convert optical energy to chemical energy (in the form of electrolytic products) and/or electrical energy. A photoelectrochemical cell is schemed in Figure 1. While metal electrodes do give photoeffects,¹⁴ semiconductor photoelectrodes have been found to give the highest quantum efficiency for electron flow in the external circuit. The greater efficiency of the semiconductor electrode can be ascribed to the longer lifetime of the photogenerated electron-hole pair, allowing redox chemistry to compete effectively with electron-hole recombination. A key fact seems to be that for semiconductors any potential drop is in the semiconductor (depletion layer) and not in the electrolyte (double layer) as for metal electrodes.

Development of a depletion layer in the semiconductor upon immersing it into an electrolyte is a consequence of the mismatch of the Fermi level of the semiconductor and the "Fermi level" of the electrolyte which is taken as the redox level.

Bending of the energy bands at the surface of the semiconductor occurs when the Fermi levels of the semiconductor and electrolyte are not the same. At equilibrium the band bending is energetically equal to the initial difference in Fermi levels, and the band bending may be favorable for observation of efficient photocurrents. Favorable band bending schemes are shown in Figure 2 for n-type and p-type semiconductors. Absorption of a photon, causing a valence band to conduction band transition within the depletion region, results in a *separated* electron-hole pair such that the *minority charge carrier* reaches the semiconductor-electrolyte interface for participation in a redox reaction. Thus, n-type semiconductors are photocathodes and dark cathodes whereas p-type materials are photoanodes and dark anodes. Fast electron transfer processes at semiconductors obtain when the redox levels overlap the appropriate band of the semiconductor. The maximum open circuit photopotential is equal to the amount of band bending and is controlled, therefore, by the electrolyte Fermi level for a given semiconductor. Thus, overall efficiency should depend significantly on the redox active substrates in the solution. The maximum theoretical efficiency is just open circuit photopotential divided by the band gap energy, but operational efficiency will depend on relative rates of electron-hole recombination and electron transfer. The foregoing understanding of semiconductor electrochemistry has been known for some time,¹⁵ and the basic principles associated with a wet photoelectrochemical cell as an energy conversion device were recently elaborated.¹⁶ This development is necessary here to discuss our new results on CdS and CdSe.

The ability to overcome electron-hole recombination by the band bending is a situation seemingly not encountered in molecular photochemistry. For example, photoexcited $\text{Ru}(\text{bpy})_3^{2+}$ is a more powerful reducing agent than the ground state species,¹⁷ but when electron transfer to a substrate occurs, generating ground state $\text{Ru}(\text{bpy})_3^{3+}$, *back electron transfer is difficult to inhibit*. For the semiconductor, though, one either has built-in inhibition of electron-hole recombination or can induce it with an appropriate applied potential from a power supply in the external circuit.

Naturally, if the objective is to convert light exclusively to electrical energy, one seeks a redox system which will induce favorable band bending without any external bias. Moreover, the redox chemistry must be such that no net chemical change occurs, i.e., what is oxidized at a n-type photoanode must be reduced at the cathode to regenerate the original electrolyte. However, if the objective is to produce chemical energy, an

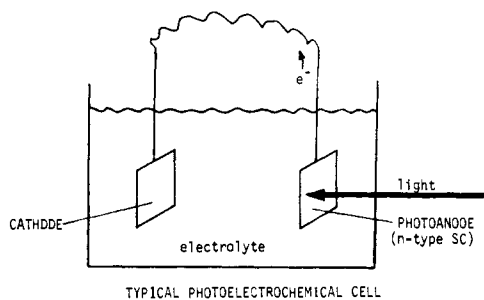


Figure 1. Typical photoelectrochemical cell.

external power supply could be used in series with the photoeffect. For example, if the electrolysis of water could be done at any potential lower than the reversible potential of 1.23 V¹⁸ by irradiating one (or both) electrodes, then optical energy would be converted to chemical energy. If the open circuit photopotential of a photoelectrochemical cell exceeds the reversible electrolysis potential of the fuel-forming reaction, then both electrical *and* chemical energy can result from the irradiation of the cell if the current passes through an external load.

Evidence of the intense interest in stable semiconductor photoelectrodes comes from the recent developments in studies of n-type metal oxide photoelectrodes. Early claims¹⁹ that TiO₂ is a stable photoanode in aqueous electrolytes were proven,²⁰ and subsequently, considerable further characterization of this system has been reported in the literature.²¹⁻³⁰ The basic finding^{19,20} is that TiO₂ is essentially indefinitely inert to photoanodic dissolution in aqueous electrolytes, but that a small external potential (~0.25 V) in series with the photoeffect is required²⁰ for the photoelectrolysis of H₂O to H₂ and O₂. More recently, SnO₂,³¹ SrTiO₃,^{32,33} KTaO₃,³⁴ and KTa_{0.77}Nb_{0.23}O₃³⁴ were found to serve as stable photoanodes in cells for the photoelectrolysis of H₂O. Importantly, the perovskite-based cells were shown^{32,34} to photoelectrolyze H₂O with no external energy source other than light. Unfortunately, all of the metal oxide semiconductors cited above have band gaps of ≥3.0 eV: TiO₂ (3.0 eV),³⁵ SnO₂ (3.5 eV),³⁶ SrTiO₃ (3.2–3.4 eV),³⁷ and KTaO₃, KTa_{0.77}Nb_{0.23}O₃ (3.5–3.6 eV).^{38,39} Thus, the stored chemical energy (1.23 eV) is only a small fraction of the light energy required to drive the reaction. Moreover, visible light responsive systems are seemingly needed if photoelectrochemical cells are to be of value in solar energy conversions.

There are many small band gap, visible light responding semiconductor photoelectrodes of the n-type, but it is just these that undergo photoanodic dissolution. In addition to the approach to be detailed here of adding a competitive redox active substance to the electrolyte, there are several other concepts being pursued to achieve visible light response and stability. First, one may attempt, by doping inherently stable materials like TiO₂,⁴⁰ to introduce new electronic transitions within the gap which produce the minority charge carrier with less than band gap energy excitation. This may suffer from low efficiency of minority charge carrier generation. This is a consequence, principally, of low absorptivity due to low maximum doping levels. Second, one may sensitize response by adsorbing dyes onto the semiconductor surface.^{41,42} According to Gerschler,¹⁶ the dye sensitization approach suffers from the fact that only monolayers of dyes are active for electron transfer which restricts light absorption to the order of 1–2%. Thicker dye layers increase the resistance of the system without adding to the current generation.¹⁶ Third, one may try coating a small band gap, unstable semiconductor with a thin, inert, transparent metal film,⁴³ hoping to have the light response of the semiconductor and the stability of a metal electrode. Similarly,

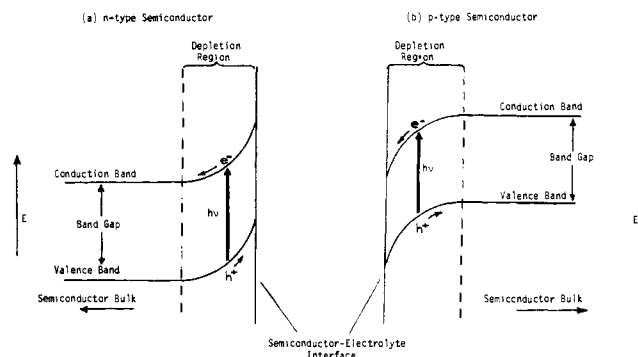


Figure 2. (a) Semiconductor–electrolyte interfacial region showing band bending favorable for observation of a photocurrent for an n-type semiconductor. (b) Same as (a) except for a p-type semiconductor.

one may coat a small band gap semiconductor, such as CdS, with a large band gap, inherently stable semiconductor such as TiO₂.⁴⁴ Coating a semiconductor with a metal is a Schottky barrier photocell and may have no inherent advantages used as an electrolysis cell. Coating a semiconductor with another semiconductor suffers, as do dye coatings and thin metal films, from removing the utter simplicity of fabricating the devices. It is apparent, too, that the approach described herein of adding a competitive redox agent is not without its disadvantages: (1) many potential redox candidates absorb strongly in the visible and (2) use of a competitive redox system removes the ability to generally drive any redox reaction. Another approach to “good”, stable, efficient photoelectrochemical cells for the conversion of optical energy is serendipity, but even this approach may be hampered by the common knowledge of the working model^{15,16} and the intense desire for visible light responding systems.

The objective of this paper is to present our results on the characterization of CdS and CdSe based photoelectrochemical cells employing alkaline sulfide or polysulfide aqueous electrolytes. While a number of studies^{4-8,45-47} have been carried out on CdS and CdSe based cells, no characterization has been reported where the electrode surface has been demonstrated to be completely stable when an anodic photocurrent is flowing. We now describe measures of stability, wavelength response, open-circuit photopotential, current–voltage properties, and overall optical to electrical energy conversion efficiencies, and we discuss these in relation to the working model outlined above.

Results and Discussion

Stability. Irradiation of either CdS or CdSe single crystal electrodes in a cell with a Pt cathode results in current such that electrons flow toward Pt. In 1.0 M NaOH as the electrolyte, the photocurrent falls very rapidly with irradiation time as shown in Figure 3, and the production of elemental sulfur on CdS or elemental selenium on CdSe is very obvious at a reasonable light intensity. By adding either Na₂S or Na₂S and S to the 1.0 M NaOH, a very stable photocurrent can be sustained by constant visible light irradiation. Figure 3 shows the dramatic difference in the photocurrent vs. time plot in 1.0 M NaOH and 1.0 M NaOH, 1.0 M Na₂S, and 1.0 M S electrolytes. We have demonstrated that sulfide is oxidized with ~100% current efficiency by monitoring electrode stability and visible spectral changes as a function of irradiation time. This oxidation completely “quenches” photoanodic dissolution of either CdS or CdSe.

In the absence of zero valent sulfur, H₂ is evolved initially at the Pt cathode. When zero valent sulfur is added (or photogenerated), H₂ evolution is quenched to some extent, dependent on current density. Presumably, the reaction occurring at the cathode in the presence of zero valent sulfur is the re-

Table I. Stability of CdS and CdSe Photoanodes

Crystal	Face ^a	Crystal, mol × 10 ⁴		Electrons generated, mol × 10 ⁴	Av i, mA ^c	Time, h
		Before	After			
CdSe	0001 ^b	9.39	9.41	4.20	0.64	17.6
	000 $\bar{1}$ ^b	8.61	8.61	3.31	0.41	21.6
	Not etched ^c	8.78	8.75	23.9	4.2	15.4
CdS	0001 ^b	6.70	6.70	2.04	1.07	5.1
	000 $\bar{1}$ ^b	6.96	6.88 ^f	1.99	0.59	9.1
	Not etched ^b	8.64	8.64	1.95	0.45	11.7
	Not etched ^d	5.53	5.44	33.8	~1.0	84.5

^a Etched according to ref 55 and 56. ^b Electrolyte is 1.0 M NaOH, 1.0 M Na₂S, and 1.0 M S. ^c Electrolyte is 1.0 M NaOH and 0.2 M Na₂S. ^d Combination of experiments carried out in either electrolyte indicated in footnote ^c or in 1.0 M NaOH, 0.2 M Na₂S, and 1.0 M S. ^e For current density multiply by 4 cm⁻². ^f This sample was etched after mounting and this is the likely source of the loss.

duction of some polysulfide species. We have found that electrolytes consisting of 1.0 M NaOH, 1.0 M Na₂S, and 1.0 M S yield no H₂ evolution at the cathode at any current density up to 20 mA/cm².

The quantitative measure of photoelectrode stability is given in Table I. The data show that substantial anodic photocurrents result in no deterioration of CdS or CdSe in the sulfide-containing electrolytes. Data are given for average current densities which range from approximately 1 to 16 mA/cm². At very high light intensities one typically observes some decline in photocurrent and some surface discoloration of the crystal, but in no case have we observed any significant weight loss in either CdS or CdSe, even after the passage of substantial current for prolonged periods.

The stability verified in Table I for CdS and CdSe is unprecedented. A more subtle, but more qualitative, measure of electrode stability should include a discussion of photocurrent stability. Generally, the photocurrent either holds constant or drops slowly with prolonged irradiation times. Interestingly, in the polysulfide electrolyte (1.0 M NaOH, 1.0 M Na₂S, and 1.0 M S), and for etched surfaces, the CdSe gives a more steady photocurrent than CdS. The photocurrent vs. time profile for the CdSe (000 $\bar{1}$) irradiation of 21.6 h in Table I represents a very stable situation: the photocurrent started at 0.405 mA and rose quickly to 0.425 mA where it held constant for 5.9 h; it then fell to 0.400 mA over the next ~7.3 h and held constant at 0.400 mA for the final 8.3 h. High light intensities seem to give less stable photocurrents on etched surfaces than on surfaces which have only been polished, but the etched surfaces give significantly larger photocurrents. Our qualitative observation is that the etched surfaces are more delicate, but at moderate light intensities for CdS and high intensities for CdSe, the sulfide- or polysulfide-containing electrolytes do quench the gross photoanodic dissolution of the electrode. The constant photocurrents suggest, but by no means prove, that the surface layer is not changing with irradiation time.

A difficult question to answer quantitatively is what is the minimum concentration of added sulfide or polysulfide that will completely quench the photoanodic dissolution. The answer, in our experiences, depends on the current density. With respect to the quantitative measurements that we have made, we can say definitively that alkaline electrolytes containing at least 0.2 M Na₂S do yield stable photoelectrodes at current densities up to 16 mA/cm².

Sensitive, but again qualitative, measures of photoelectrode integrity include constancy of current-voltage properties for a given photoelectrode and constancy of wavelength response for CdSe. These measurements are detailed below, but their essential features are constant before and after prolonged irradiation in the polysulfide electrolyte. Especially for CdSe, these observations rule out any significant exchange according to reaction 3.

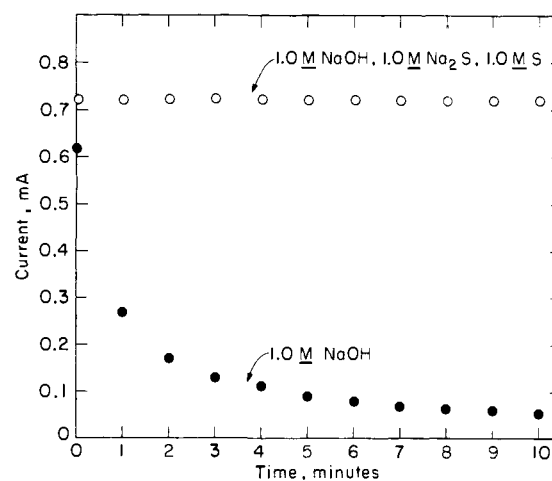


Figure 3. Photocurrent as a function of time in a CdSe based cell using 1 M NaOH as an electrolyte (●) or using an electrolyte consisting of 1 M NaOH, 1 M Na₂S, and 1 M S (○). The irradiation source is a beam-expanded He-Ne laser with output at 633 nm. The 0001 face of the crystal is exposed to the electrolyte.



In principle, this exchange could occur photochemically or in the dark, but we do not find that CdSe develops properties similar to CdS. Some surface exchange may occur according to reaction 3, but we *do not* observe the color change (black to yellow), the wavelength response onset change (~750 to 520 nm), or changes in current-voltage properties that would reflect any significant amount of the exchange.

The remarkable stabilizing power of the sulfide or polysulfide is surprising in view of the fact that several other additives to electrolytes are only competitively oxidized at CdS or CdSe photoanodes.⁷⁻¹⁰ Phenomenologically, sulfide is simply scavenging photogenerated surface holes at rates which swamp hole consumption associated with photoanodic dissolution. Fast rates of electron transfer from the sulfide or polysulfide in the electrolyte to the electrode suggest a special interaction of the sulfide or polysulfide with the electrode surface. Such an interaction especially seems reasonable in view of the fact that high concentrations of I⁻ or Fe(CN)₆⁴⁻ do not completely quench electrode decomposition, despite the fact that I⁻ and Fe(CN)₆⁴⁻ both have oxidation potentials which are seemingly in the proper energy range. The early suggestion¹¹ that S²⁻ might quench the photoanodic dissolution of CdS seems based on what might be termed a symbiotic effect. That is, S²⁻ or S_n²⁻ is oxidized very rapidly at CdS (or CdSe) compared to I⁻, Fe(CN)₆⁴⁻, and the like because S²⁻ and S_n²⁻ have a special affinity for the electrode surface. This proposition is plausible, since it is well appreciated that differences in elec-

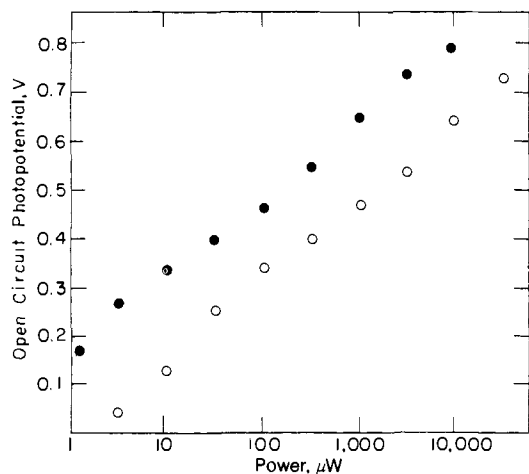


Figure 4. Plot of open circuit photopotential against light intensity at 514.5 nm (○) and 501.7 nm (●) for CdS based cell with a 1 M NaOH, 1 M Na₂S, and 1 M S electrolyte. The 0001 face (0.25 cm²) is exposed. Potential values shown are between Pt and CdS.

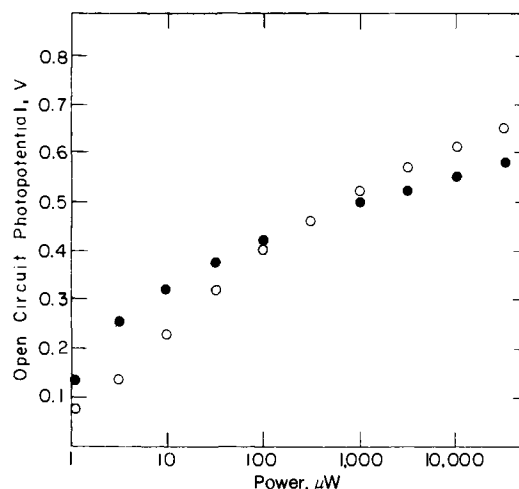


Figure 5. Plot of open circuit photopotential against light intensity (514.5 nm) for CdSe based cell with a 1 M NaOH, 1 M Na₂S, and 1 M S electrolyte. Open circles are for the 0001 face and filled circles are for the 0001 face of the crystal exposed to the electrolyte. Potential values shown are between Pt and CdSe.

trochemical oxidation rates can exist for species having very similar potentials. The fact that the reaction being quenched is electrode decomposition seems to demand extraordinary circumstances, since the photoanodic dissolution of the electrode is not controlled by diffusion. Mass transport controlled S_n^{2-} oxidation, which may be the case at high enough light intensity, offers a rationale for the prospect of facing dissolution problems at very high light intensities.

We have already mentioned the qualitative results from "etching". It is important to recognize that etching distinguishes the 0001 and 0001 faces of the CdS and CdSe crystals. The 0001 face is principally Cd, and the 0001 face has principally S or Se exposed. It has been claimed⁴⁸ that the face which is exposed can have some measurable influence on the photoelectrochemical behavior. In our experiments we have shown that stability obtains for either the 0001 or 0001 face, Table I.

For etched samples and at sufficiently high intensity we do often observe some decline in photocurrent, but there is no overall photoanodic dissolution. The decline in photocurrent is especially found for CdS based cells. For example, we have seen ~25% decline in photocurrent over a period of time long enough to consume ~25% of the CdS with no detectable weight loss. We ascribe the declining photocurrent to subtle changes in surface structure of CdS. Given this apparent reorganization of the electrode surface for CdS, it may be plausible to propose that photoanodic dissolution may occur to some extent, but that it is more or less reversed by the instantaneous precipitation of CdS by reaction of the released Cd²⁺ and the S²⁻ or S_n^{2-} of the electrolyte. This mechanism for stability is unsatisfactory for CdSe because of the lack of the black to yellow color change that would be expected if CdS were precipitated to regenerate the electrode.

Open Circuit Photopotential. Both CdS and CdSe are known to produce large open circuit photopotentials. A recent article¹⁶ shows values for CdS up to about 1.25 V and for CdSe up to about 0.75 V. We have measured the open circuit photopotential for both CdS and CdSe as a function of light intensity. Typical results are shown in Figures 4 and 5 for the electrolyte consisting of 1.0 M NaOH, 1.0 M Na₂S, and 1.0 M S. The potentials measured are those between the Pt and the photoelectrode.

In accord with theory¹⁵ the open circuit photopotential depends linearly on the log of the light intensity over several orders of magnitude. For CdS the measurement has been made for an excitation wavelength which is just on the absorption

edge (514.5 nm) and for a value at slightly higher energy (501.7 nm). For 514.5 nm, according to the wavelength response curves (vide infra), the maximum photoeffect does not obtain, whereas 501.7 nm is a wavelength very close to the maximum response. The point is, at an equal incident intensity the 501.7 nm irradiation is more effective than the 514.5 nm. The open circuit photopotentials given in Figure 4 reflect this expectation rather nicely. The higher absorptivity at 501.7 nm results in a greater fraction of the incident light being absorbed within the depletion layer. Since the same slopes obtain for the plots at both 501.7 and 514.5 nm irradiation, we can conclude that the fraction of useful light absorbed at 501.7 nm is about 10 times greater than that from an equivalent incident intensity at 514.5 nm. This factor is in reasonable agreement with the relative photocurrent at short circuit from an equal intensity irradiation at 501.7 and 514.5 nm as judged from the wavelength response curves. Comparable, but not exactly the same, photopotential values are obtained from crystal to crystal of CdS. Additionally, we have not been able to distinguish a reliable difference between the 0001 and 0001 face of either CdS or CdSe. Data for the 0001 and 0001 face of a CdSe photoelectrode are given in Figure 5. The differences shown are comparable to the variations from sample to sample.

Comparing the data in Figures 4 and 5, we see that photopotentials on CdS at a given intensity are somewhat higher and the saturation effect sets in at a higher intensity compared to the CdSe. Qualitatively, these trends are as found¹⁶ in a different electrolyte.⁴⁹ We examined the open circuit photopotentials in 1.0 M NaOH and found values similar to those obtained in the 1.0 M NaOH, 1.0 M Na₂S, and 1.0 M S electrolyte. In practical terms, the invariance of the open circuit photopotential between these two electrolytes means that by stabilizing the electrode to photoanodic dissolution by adding S_n^{2-} one does not significantly change the expected energy conversion efficiency.

Wavelength Response Curves. Relative photocurrent as a function of excitation wavelength at a constant number of photons incident on the electrode is shown in Figures 6 and 7 for CdS and CdSe, respectively. The data are reported for the 1.0 M NaOH, 1.0 M Na₂S electrolyte which is transparent over the range of interest. As expected, lower than band gap excitation is largely ineffective, but for wavelengths shorter than band gap, response is observed. Included in the figures is the optical density for a polished 1 mm thick sample of CdS and CdSe. The sharp increase in absorbance which occurs at

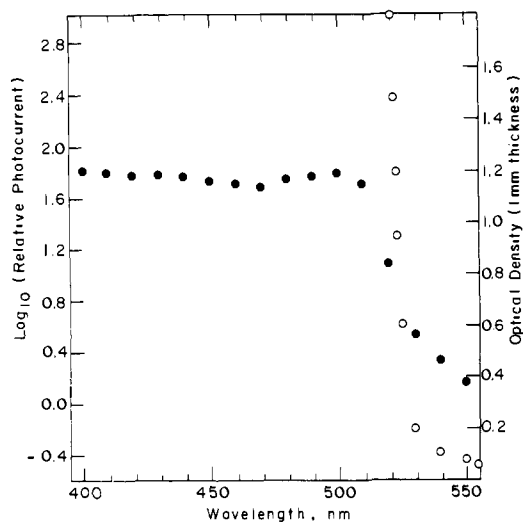


Figure 6. Wavelength response curve (●) for CdS based cell and absorption (○) of a 1 mm thick polished CdS crystal. The wavelength response has been corrected for variation in light intensity as a function of wavelength. The electrolyte is 1.0 M Na₂S and 1.0 M NaOH.

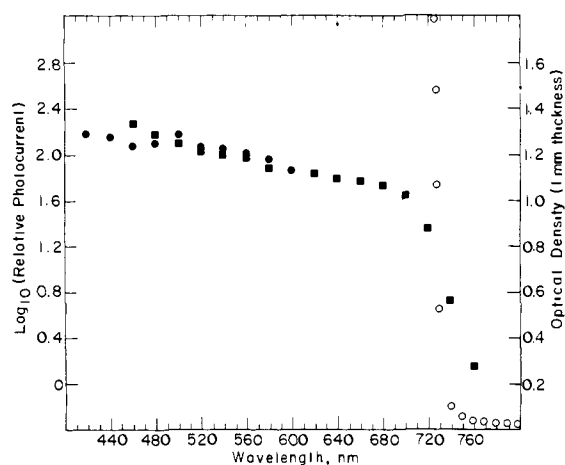


Figure 7. Wavelength response curve for a CdSe based photoelectrochemical cell with a 1 M NaOH and 1 M Na₂S electrolyte. The filled circles (●) and squares (■) are relative photocurrents as a function of incident irradiation wavelength after correction for variation in intensity with wavelength. The filled circles were values obtained using the excitation optics of an Aminco-Bowman emission spectrophotometer as the irradiation source, and the filled squares are values using a 600 W tungsten source monochromatized using a Bausch & Lomb high intensity monochromator. The open circles are the optical density for a 1 mm thick polished CdSe crystal.

the known⁵⁰ band gap of the semiconductors corresponds to the photocurrent onset. For CdS, wavelengths significantly shorter than band gap energy give essentially constant response. By way of contrast, we typically find that the response increases gently for CdSe with increasing excitation energy. For example, the response at ~450 nm is about two times greater than at ~630 nm. We can offer at least one explanation for this effect: the fraction of incident light absorbed within the depletion layer is greater at the higher excitation wavelengths. This could be due to inherently higher absorptivity at the shorter wavelengths. Alternatively, the increased absorption could be due, in part, to greater scattering of the incident beam at the shorter wavelengths, as expected for a matte-like surface.

Current-Voltage Properties. Current-voltage properties for CdS and CdSe electrodes have been measured with a standard three-electrode cell and a potentiostat. A saturated calomel electrode (SCE) was used as a reference electrode. Current-

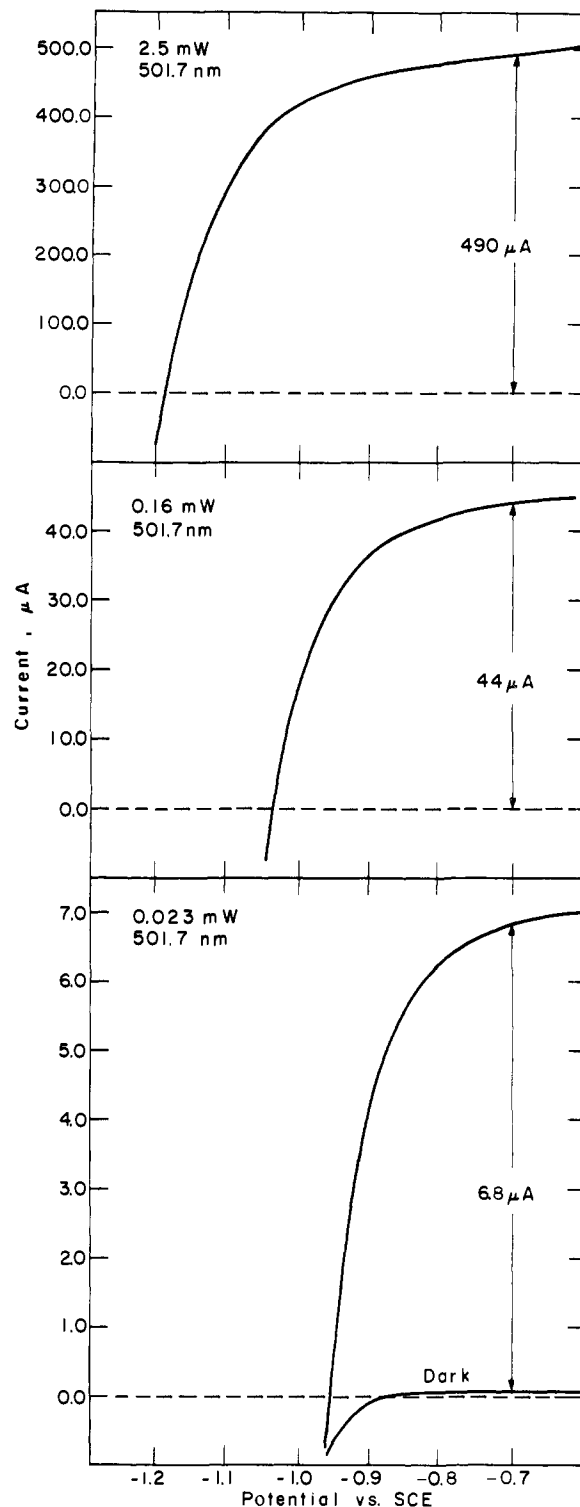


Figure 8. Current-voltage properties for an irradiated (501.7 nm) n-type CdS (0.25 cm² surface area) electrode. The 0001 face is exposed to the 1.0 M NaOH, 1.0 M Na₂S, and 1.0 M S electrolyte. The Pt dark electrode potential was constant at -0.71 V vs. SCE for any bias. The sweep rate for all curves is 0.2 V min. Note the dependence of the curves on irradiation power.

voltage curves for CdS and CdSe under comparable conditions are given in Figures 8 and 9 for three different light intensities in the 1.0 M NaOH, 1.0 M Na₂S, and 1.0 M S electrolyte. For all situations given here the Pt potential was measured to be invariant in a given electrolyte and only the photoelectrode potential changed in the bias range used. First, the dark anodic current was either small or nonexistent in every case, consistent with the lack of holes available at the surface for participation

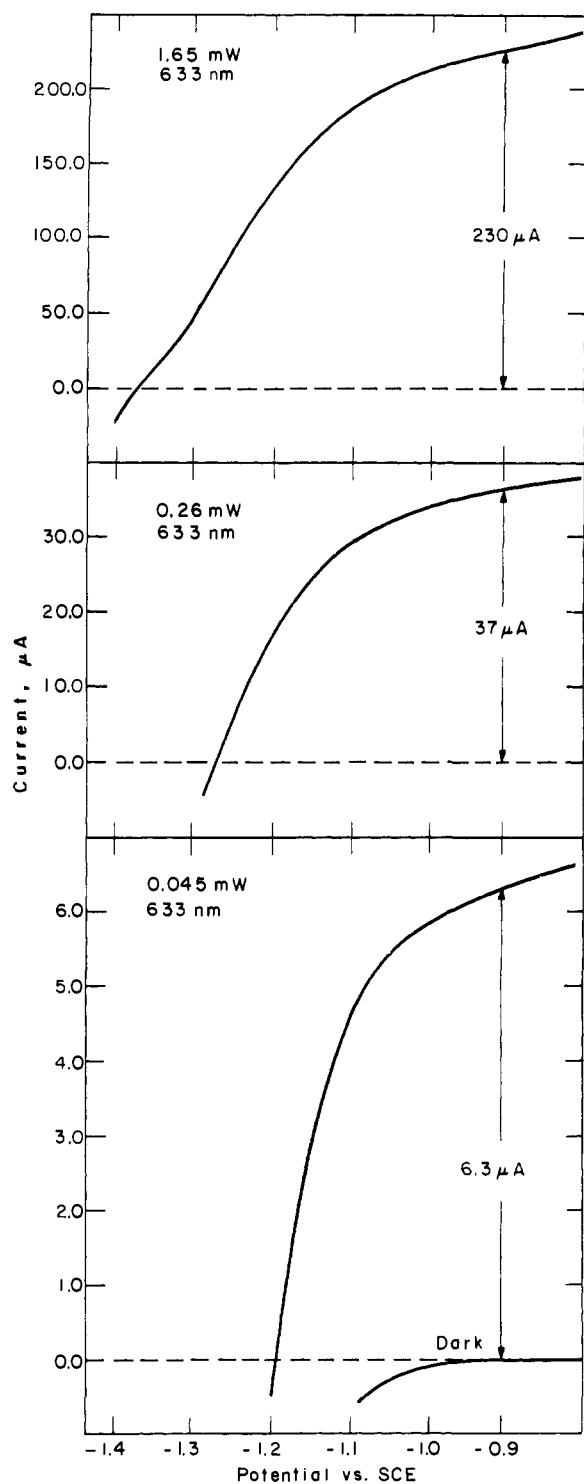


Figure 9. Current-voltage properties for an irradiated (633 nm) n-type CdSe (0.25 cm² surface area) electrode with 0001 face exposed to the 1.0 M NaOH, 1.0 M Na₂S, and 1.0 M S electrolyte. The Pt dark electrode potential was constant at -0.71 V vs. SCE for any bias. The sweep rate for all curves is 0.2 V/min. Note the dependence of the curves on irradiation power.

in the electron transfer. Dark cathodic currents are observed, since there are electrons available without irradiation. At a sufficiently large anodic bias, irradiation yields the generation of holes which can then lead to the photoanodic current. As seen in Figures 8 and 9, the onset of the photoanodic current moves more negative with increasing light intensity in a manner consistent with the value of the open circuit photopotential as a function of light intensity. That is, with an order of magnitude increase in light intensity, the photoanodic onset

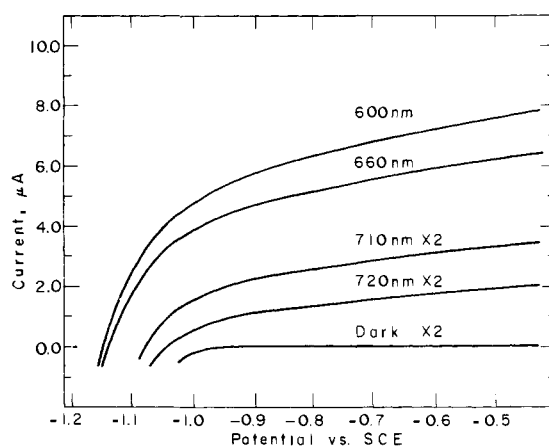


Figure 10. Current-voltage properties of CdSe as a function of incident irradiation wavelength. The 0001 face, 0.25 cm² surface area, is exposed to the 1.0 M NaOH, 1.0 M Na₂S, and 1.0 M S electrolyte and illuminated at a constant intensity of 7.2×10^{-10} einstein/s at all four wavelengths. The Pt dark cathode potential was constant at -0.72 V vs. SCE, and the sweep rate was 0.2 V/min.

shifts more negative by about 0.15 V. The fact that the photocurrent onset is more negative than the Pt electrode potential means that the conversion of light energy to electrical energy is possible.

While electricity may be generated at a higher voltage for the higher intensities, the current-voltage behavior for CdS as a function of light intensity shows that the maximum photocurrent is not directly proportional to light intensity for the highest light intensities. For the three intensities measured we have a ratio of currents at -0.7V vs. SCE (1:6.47:72.06) while the ratio of intensities was (1:6.95:108.7), reflecting an approximately 30% lower quantum efficiency at the highest light intensity compared to the lowest intensity. For a slightly smaller range of intensities for CdSe, the ratio of currents at -0.9 V vs. SCE is (1:5.87:36.5) while the ratio of intensities is (1:5.78:36.6). This illustrates a range of intensities for which saturation does not obtain. However, at a sufficiently high intensity the CdSe based system also saturates. In fact, it can be appreciated that the choice of the potential where the photocurrent is taken (-0.7 V for CdS and -0.9 V for CdSe) is somewhat arbitrary. We have, although, attempted to record the photocurrent as a function of intensity at a potential where the current is reasonably insensitive to the potential.

Current-voltage properties for both CdS and CdSe have been measured as a function of excitation wavelength. In neither case do we find a major change in the essential voltage dependence of the current, for excitation wavelengths shorter than band gap energy. In the region near band gap, though, we do find an interesting wavelength dependence. A typical set of current-voltage curves at different excitation wavelengths, but same intensities, are shown in Figure 10 for CdSe. In this case we find that the photoresponse has its onset near 750 nm. Decreasing the excitation wavelength, but holding the light intensity constant, the maximum photocurrent increases and the anodic photocurrent onset is more negative. The more negative onset is wholly consistent with the notion that a higher effective light intensity obtains at the shorter excitation wavelengths. We attribute the effect to the differing penetration depth of the light in the wavelength region of the absorption edge which results in a different amount of light absorbed within the depletion region. This is the same argument offered to explain the difference in open circuit photopotential at 501.7 and 514.5 nm for CdS for equal intensity incident on the electrode.

As with all the measures of characterization, we have attempted to distinguish a difference in the current-voltage

properties of electrodes with either the 0001 or 000 $\bar{1}$ face exposed. We cannot at this time report a real difference, though it may be expected to exist. We ascribe our irreproducibility for a given face to large differences in the extent of etching from sample to sample. Etching causes remarkable changes in current-voltage properties in the "as received" crystals, but we have generally been unable to reproduce the surfaces by the etching procedures used. For example, we have contented ourselves with anodic onsets which are within 100 mV of one another for two different crystals with the same face exposed. This error seems to cloud any differences in the 0001 and 000 $\bar{1}$ face.

A final parameter that we have investigated with respect to current-voltage properties is electrolyte composition. We measured current-voltage curves at 0.045 (633 nm) and 1.65 mW (633 nm) for CdSe for several different 1.0 M NaOH electrolytes having variable amounts of added S and Na₂S. The S concentration ranged from 0.05 up to 1.0 M and the Na₂S concentration ranged from 0.2 to 1.0 M. In all cases the low intensity curves were very comparable. However, at the high light intensity the solutions containing a smaller amount of total sulfur gave substantial differences. The differences were mainly that the photocurrent saturates at the higher intensity and there is a less steep increase in the photocurrent with increasing anodic bias. A comparison of two electrolytes is shown in Figure 11. This suggests that the distribution of S_n²⁻ species present is crucial to obtaining optimal current-voltage properties. We regard "optimal" as those curves displaying the most negative anodic current onset, the most steeply rising photocurrent with increasing anodic bias, and the most linear response of photocurrent with light intensity.

Overall Energy Conversion Efficiency. Photoanodic current onsets which are more negative than the cathode potential and photoelectrode stability indicate that it is possible to use the system to sustain conversion of light energy to electrical energy. Additionally, though, it is appropriate to prove that the electrolyte itself is not being consumed in the process. That is, we need to demonstrate that prolonged photocurrent flow does not lead to deterioration of the electrolyte. The arbitrary use of the 1.0 M NaOH, 1.0 M Na₂S, and 1.0 M S electrolyte for all energy conversion measurements seems justified in view of the optimal current-voltage properties obtained in this electrolyte. Incidentally, prolonged irradiation of the electrolyte itself results in no discernible changes.

To prove that the electrolyte is undergoing no net chemical change upon prolonged current flow we measured the optical absorption spectral changes accompanying electrolysis. An Ar purged 2.0 cm³ solution of 1.0 M NaOH, 1.0 M Na₂S, and 1.0 M S was electrolyzed at a constant potential of 0.5 V yielding ~2.0 mA of current. Two Pt-gauze electrodes (~1 cm² in area) were used, and the positive lead of the power supply was connected to one electrode and the negative lead to the other. The electrolysis was carried out in a sealed, 0.1 mm path length cuvette for a period of ~40 h. First, a constant current was observed. This indicates that the electrochemically active species at the potential used are not depleted in time. Monitoring the absorption spectrum in the range 700–350 nm revealed a small amount of redistribution of the polysulfide species during the first portion of the electrolysis. But at least during the last 20 h of electrolysis no spectral changes occurred. Moreover, after the electrolysis was complete, the solution regained its original spectrum upon standing for several hours. Apparently, these spectral changes correspond to the thermal regeneration of the original distribution of polysulfide species. The largest reversible change in optical density was approximately 20% of the original value at 350 nm. During the electrolysis enough electrical equivalents passed to substantially consume the redox active polysulfide. The possible culprit in the polysulfide system is irreversible oxygenation. But it is

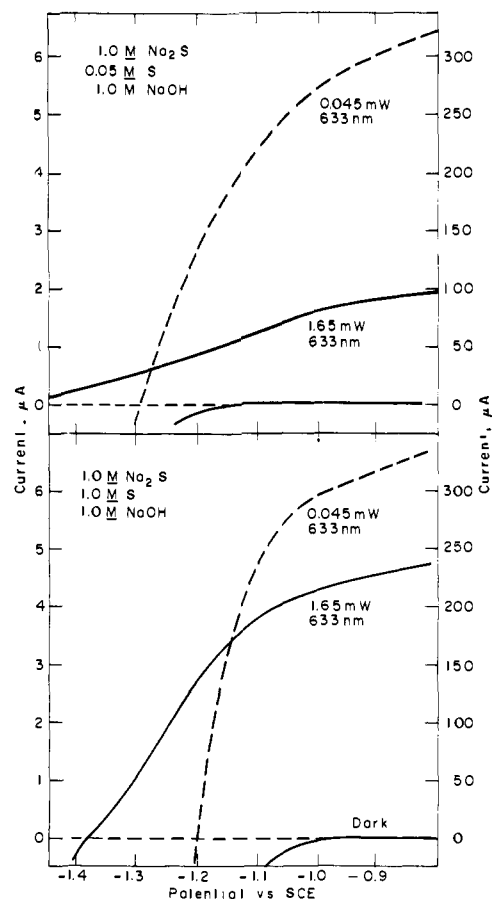
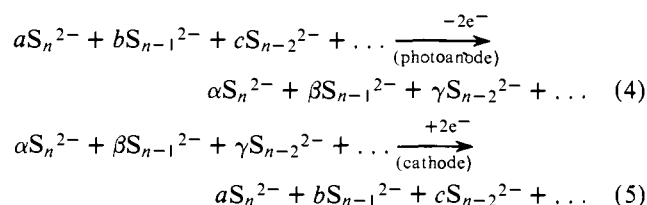


Figure 11. Dependence of CdSe current-voltage properties on intensity and electrolyte composition. In each case the sweep rate was 0.2 V/min and the 0.25 cm² 0001 surface is exposed. In the 0.05 M S electrolyte the Pt electrode is at -0.78 V vs. SCE and in the 1.0 M S electrolyte the Pt electrode is at -0.71 V vs. SCE.

known⁵¹ that this only occurs at fairly large potential and high current density, neither of which obtains in the CdS or CdSe based cell. Similarly, using either CdS or CdSe based photoelectrochemical cells we have sustained sizable photocurrents in 2.0 cm³ electrolytes for periods long enough to observe significant changes in electrolyte composition. Not only do we not see decomposition of the electrolyte, but we have also observed steady photocurrents for constant illumination intensity. We have not placed these observations on a wholly quantitative footing, but the conventional electrolysis results described above, and our numerous experiences with CdS and CdSe in polysulfide, convince us that the electrolyte does not undergo any net, irreversible chemical change. One may well change the distribution of polysulfides, but no deleterious effects result. Thus, for 1.0 M NaOH, 1.0 M Na₂S, and 1.0 M S we have a situation as summarized in eq 4 and 5.



We cannot specify precisely the coefficients n , a , b , c , α , β , γ , etc., since they will depend on the concentration of S, Na₂S, and the base strength.⁵² The point is, however, that the oxidation of polysulfides is effectively reversed at the cathode.

Two other practical aspects concerning the polysulfide electrolyte and overall energy conversion need to be discussed at this point. First, the polysulfides are air sensitive, and we

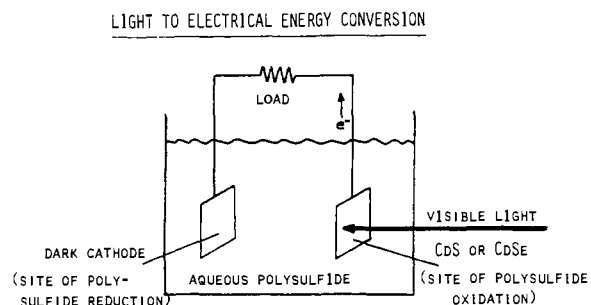


Figure 12. Schematic representation of n-type CdS and CdSe based photoelectrochemical cells. Photoanodic dissolution of CdS(e) does not occur in the aqueous polysulfide electrolyte, rather the polysulfide is oxidized at the photoelectrode.

have consistently used continuously Ar purged electrolytes in all studies of overall energy conversion efficiency. Thus, all results are reported herein for stirred, rather than quiet, solutions. The second point that should be raised is that the polysulfide electrolyte absorbs in the visible region of the spectrum. For a 1 mm path length of the 1.0 M NaOH, 1.0 M Na₂S, and 1.0 M S electrolyte, the optical density is ~1.0 at 490 nm; and for a 0.1 mm path length the optical density is ~1.0 at 400 nm. Thus, especially for CdS based cells which have an onset near 520 nm, there is considerable absorption by the electrolyte in wavelength ranges of interest. Consequently, we have made all power conversion efficiency measurements at longer wavelengths than the absorption onset of the electrolyte.

We have made measures of power conversion in a cell as schemed in Figure 12. The "load" in series in the external circuit has been a variable power supply. Recall that a positive bias will assist oxidations at the photoelectrode. A negative bias ("−" lead to CdS or CdSe, "+" lead to cathode) will "resist" the flow of an anodic photocurrent, and the power supply then represents a load in the external circuit. At any negative applied potential where an anodic photocurrent can be observed, the cell is actually producing electric power. Power output is equal to the photocurrent times the negative applied potential. The maximum power output for a given input light power can be easily determined from a plot of photocurrent vs. applied potential from the power supply. One simply finds the maximum value of the product of current and voltage. Representative plots of photocurrent against applied potential are given in Figure 13 for both the CdS and the CdSe based cells. The applied potential axis is just the difference in potential between the cathode and the photoelectrode supplied by the power supply. For the plots shown there is a considerable amount of photocurrent at negative applied potentials indicating substantial electrical power output. Incidentally, we have measured identical power conversion by replacing the power supply with a resistor in series in the external circuit where the power output is then just the (current)² times resistance.

The maximum efficiency for conversion of light energy to electrical energy, η_{\max} in percent, is given by eq 6.

$$\eta_{\max} = \frac{(\text{current} \times \text{potential})_{\max}}{\text{optical power in}} \times 100 \quad (6)$$

At low light intensities we have measured η_{\max} values as high as 9.2% for CdSe, irradiating at 632.8 nm. This electrical power output occurs at a potential of 0.35 V, Figure 13. Likewise at low light intensities we have measured η_{\max} values as high as 6.8% for CdS at 500 nm and 0.30 V, Figure 13.

Table II summarizes our several measures of optical to electrical energy conversion using CdS and CdSe based photoelectrochemical cells. In all cases the power conversion ef-

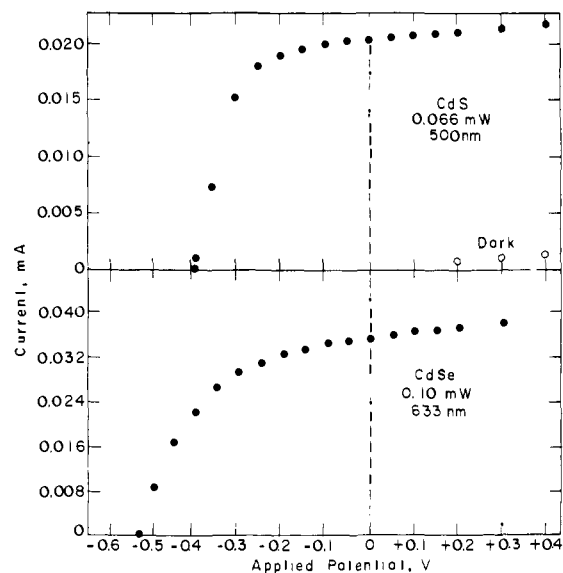


Figure 13. Photocurrent vs. applied potential from a power supply in series in the external circuit of the CdS and CdSe based cell. The electrolyte is 1 M NaOH, 1 M Na₂S, and 1 M S. At any negative applied potential the power supply represents the "load" in Figure 12 and there is a positive efficiency for the conversion of light to electricity. Data as shown here were used to give the efficiencies in Tables II and III. These two plots are for experiments No. VIII (CdS) and V (CdSe) in Tables II and III.

iciencies reported represent actual measurements, not estimates. And in several instances positive optical energy conversions have been sustained at high enough values and for long enough periods to consume a significant fraction of the photoelectrode, if it were undergoing photoanodic dissolution. Indeed, all of the data for etched sample stability (Table I) are for a situation where the power output of the cell is at a few percent efficiency (power out ~1 mW/cm² exposed area). Thus, not only are CdS and CdSe stable under anodic bias, but they are stable to photoanodic dissolution when the cells are actually yielding electrical power.

Data in Table II provide compelling evidence that both CdS and CdSe based cells give best conversion efficiencies at the lower light intensities. It appears, in fact, that at input power densities exceeding ~4 mW/cm² for CdS, and perhaps a little higher for CdSe, the power conversion efficiency suffers. The higher intensities do, however, yield maximum power output at a higher potential. Nonetheless, the efficiency suffers at the high light intensities, because we see a saturation of the photocurrent reflected in the smaller quantum efficiency for electron flow, Φ_e , at the higher light intensity.

Power conversion efficiency does vary from sample to sample. However, obtaining a sustained conversion efficiency of at least ~5% has proved to be no problem whatsoever. An extreme difference in conversion efficiency is obtained for etched vs. nonetched samples. Etching appears to improve the efficiency by about an order of magnitude. We again distinguish no substantial difference in 0001 vs. 000 $\bar{1}$ faces for these measures of overall conversion efficiency.

During the course of our power conversion efficiency measurements on CdS (but not CdSe) at high light intensities, we noted a difference in initial photocurrent stability depending on the applied potential. As the light intensity was increased, a greater load had to be put into the external circuit to achieve stable (nondeclining) photocurrents. In the case where the load was the power supply, a greater negative bias had to be applied to achieve an initially level photocurrent. The maximum value of the power conversion efficiency was always observed to occur at a potential where the photocurrent is stable. At potentials, though, where the current falls we observed no weight

Table II. Overall Energy Conversion Efficiency for CdS and CdSe Based Photoelectrochemical Cells^a

Expt ^b No.	Crystal ^c	Face ^d	Irrdn λ , nm (power, mW) ^e	Max power out, mW ^e	η_{\max} , % ^f	Potential at η_{\max} , V	$\Phi \pm 15\%$ at η_{\max} ^g
I	CdSe	Not etched	632.8 (2.2)	0.0082	0.36	-0.20	0.04
II	CdS	Not etched	501.7 (2.4)	0.0056	0.23	-0.35	0.02
III ^h	CdSe	HCl etch ⁱ	610 (0.027)	0.0012	4.3	-0.25	0.36
			(0.134)	0.0067	5.0	-0.30	0.34
			(0.760)	0.0258	3.4	-0.35	0.20
			(2.30)	0.0460	2.0	-0.35	0.12
			(6.85)	0.0664	0.97	-0.35	0.06
			(22.85)	0.0968	0.43	-0.40	0.02
IV	CdSe	0001	514.5 (0.025)	0.0012	4.8	-0.35	0.33
			(0.30)	0.0176	5.9	-0.45	0.31
			(2.5)	0.115	4.5	-0.50	0.28
			(7.3)	0.176	2.4	-0.55	0.11
V	CdSe	0001	632.8 (0.10)	0.0092	9.2	-0.35	0.52
			(2.8)	0.168	6.0	-0.35	0.33
VI	CdSe	000 $\bar{1}$	632.8 (0.10)	0.0053	5.3	-0.35	0.30
			(2.8)	0.117	4.2	-0.35	0.23
VII	CdS	0001	501.7 (0.043)	0.0019	4.5	-0.25	0.44
			(0.086)	0.0037	4.3	-0.30	0.36
			(0.129)	0.0060	4.7	-0.30	0.38
			(0.284)	0.0130	4.4	-0.35	0.31
			(0.860)	0.0310	3.6	-0.40	0.22
			(1.86)	0.0590	3.2	-0.40	0.20
			(3.44)	0.0929	2.7	-0.40	0.17
			(6.88)	0.121	2.1	-0.50	0.10
			(12.0)	0.207	1.7	-0.45	0.10
VIII	CdS	000 $\bar{1}$	501.7 (0.066)	0.0045	6.8	-0.30	0.59
IX	CdS	000 $\bar{1}$	501.7 (0.043)	0.0025	5.7	-0.25	0.56
			(0.90)	0.048	5.6	-0.30	0.44

^a Electrolyte in all cases is 1.0 M NaOH, 1.0 M Na₂S, and 1.0 M S. The circuit is as schemed in Figure 12. The load is a power supply in series in the external circuit with the negative lead to the photoelectrode, cf. text. The values for 501.7 nm irradiation have not been corrected for a small amount (<15%) of electrolyte absorption. ^b Expt No. is also keyed to Table III. ^c Each Expt No. corresponds to a different crystal. ^d The face exposed is 5 × 5 mm and the crystals are 1 mm thick, cf. Experimental Section for etching procedure. ^e Multiply by 4 cm⁻² to obtain mW/cm² except where noted. ^f Maximum optical to electrical energy conversion efficiency. These are not corrected for cell resistances or surface reflection. ^g Quantum efficiency for electron flow at the potential of the maximum energy conversion efficiency. ^h This experiment differs from the others in that the 610 nm irradiation does not uniformly irradiate the exposed surface. In fact, a smaller area was irradiated giving higher power densities. ⁱ Etching with HCl only does not completely reveal 0001 or 000 $\bar{1}$ face, cf. Experimental Section.

loss in the crystal, indicating overall stability. But we strongly suspect some surface structural change, since when the current falls, say 25% in a period of irradiation corresponding to ~25% of the electrical equivalents needed to destroy the CdS, we also see a ~25% drop in the photocurrent at potentials where the photocurrent is initially stable. These results reinforce our statements concerning relative rates of polysulfide oxidation and photoanodic dissolution of the CdS. The data simply show that the light intensity effects are a function of applied potential as well.

Inefficiency in power conversion is largely a consequence of the fact that we do not observe a unit quantum efficiency for electron flow at a negative bias equal to the band gap energy. The lack of such an ideal situation is a consequence of saturation effects on photocurrent at high light intensity and the fact that the band bending is not as large as the band gap. Table III summarizes several measures of Φ_e under various conditions. First, absolute quantum efficiency determinations as a function of wavelength accord well with the wavelength response curves. For example, the 514.5 nm observed quantum yield for CdS is about an order of magnitude lower than the values at 454.5 and 501.7 nm. Thus, these values agree with the plot of relative photoresponse as a function of wavelength. Likewise, 632.8 and 454.5 nm yields for CdSe differ only by about a factor of 2 as expected from the wavelength response curve. The observed quantum yield for electron flow is obviously a function of applied potential. Generally, the potential at which one obtains η_{\max} is not the potential where one observes the maximum quantum yield for electron flow, Table

III. Presumably, the effect of the increased anodic bias is to favorably affect band bending in such a way as to more effectively inhibit electron-hole recombination, allowing electron transfer to occur more competitively. At all but the highest light intensities, though, the value of Φ_e at η_{\max} is a healthy fraction of the maximum value of Φ_e .

The highest values of Φ_e that we have actually measured are unity within experimental error. However, in some cases others have observed quantum yields which approach two.^{45,46} This is a consequence of the ability of the primary product of the oxidation to inject an electron into the conduction band to complete a *two*-electron oxidation. From our data, though, we have no evidence for the appearance of *two* electrons in the external circuit by the absorption of *one* photon.

Summary

Data presented show that both CdS and CdSe can be stabilized to photoanodic dissolution in electrolytes containing sulfide or polysulfide. Importantly, large open circuit photopotentials are possible for both the CdS and CdSe based cells, and high quantum yields for electron flow can be obtained under conditions where the photoelectrochemical cells are actually converting light energy to electrical energy. Conversion efficiency is easily ~5% for monochromatic excitation, and the maximum electrical output occurs with a potential of a few tenths of a volt.

The promising properties of CdS and CdSe based cells mentioned above are offset by several facts: (1) conversion efficiency suffers at high light intensity; (2) photocurrent in-

Table III. Light Intensity, Wavelength, and Potential Dependence of Quantum Efficiency for Electron Flow for CdS and CdSe Based Cells^a

Expt No.	Crystal	Face ^d	Irrdn λ , nm (einstein/s) ^e	Applied potential, V ^f	$\Phi_e \pm 15\%$ ^g
I ^b	CdSe	Not etched	632.8 (1.2×10^{-8})	-0.20	0.04
II ^b	CdS	Not etched	501.7 (1.0×10^{-8})	+0.50	0.17
V ^b	CdSe	0001	632.8 (5.3×10^{-10}) (1.5×10^{-8})	-0.35	0.02
				+1.00	0.06
				-0.35	0.52
VI ^b	CdSe	000 $\bar{1}$	632.8 (5.3×10^{-10}) (1.5×10^{-8})	+0.40	0.77
				-0.35	0.33
				+0.40	0.55
IX ^b	CdS	000 $\bar{1}$	501.7 (1.8×10^{-10}) (3.8×10^{-9})	-0.35	0.30
				+0.40	0.50
				-0.35	0.23
X ^c	CdS	0001	514.5 (8.7×10^{-10}) 501.7 (7.9×10^{-10}) 454.5 (8.3×10^{-10})	+0.40	0.38
				-0.25	0.56
				+0.40	0.92
XI ^c	CdS	000 $\bar{1}$	514.5 (1.1×10^{-9}) 501.7 (9.6×10^{-10}) 454.5 (1.3×10^{-9})	-0.30	0.44
				+0.40	0.73
				+0.75	0.08
XII ^c	CdSe	0001	632.8 (1.1×10^{-9}) 454.5 (6.7×10^{-10})	+1.00	1.01
				+1.00	1.07
				+1.00	0.17
XIII ^c	CdSe	000 $\bar{1}$	632.8 (1.1×10^{-9}) 454.5 (6.7×10^{-10})	+1.00	1.17
				+1.00	1.23
				+1.00	0.53
				+1.00	0.90
				+1.00	0.34
				+1.00	0.67

^a Circuit is as schemed in Figure 12 with a power supply in series in the external circuit. ^b Electrolyte is 1.0 M NaOH, 1.0 M Na₂S, and 1.0 M S. ^c Electrolyte is 1.0 M NaOH and 1.0 M Na₂S. ^d Cf. footnote d, Table II. ^e Multiply by 4 cm⁻² to obtain einstein/s/cm². ^f Applied potential (between cathode and photoanode) using power supply in series in external circuit. Negative potential indicates that the negative lead of the power supply is attached to the photoelectrode, and positive potential indicates that the positive lead of the power supply is attached to the photoelectrode. ^g Quantum efficiency for electron flow. These values are uncorrected for a small amount (<15%) of absorption at 501.7 nm for the 1.0 M NaOH, 1.0 M Na₂S, and 1.0 M S electrolyte.

stability at high intensity reflects some surface structural changes for etched surfaces at high light intensities; and (3) the polysulfide electrolyte absorbs over a substantial fraction of the high energy portion of the visible spectrum.

Nonetheless, the results presented here are the first to show that a low energy visible light responding (onset at 1.7 eV for CdSe and 2.4 eV for CdS) photoelectrochemical cell can sustain the conversion of light to electricity with good efficiency. In fact, we estimate by using CdSe based cells that ~2% of the solar insolation at the earth's surface could be converted to electricity.⁵³ We hasten to point out, though, that single crystal photoelectrodes have been used exclusively in this work, and any practical devices would seemingly have to be based on polycrystalline electrodes. We are currently investigating the photoelectrochemical stability of such electrodes. Encouragement in this regard comes from the fact that thin film, polycrystalline SnO₂⁵⁴ and TiO₂^{22,29} and hot pressed pellet³³ SrTiO₃ based photoelectrochemical cells do work with properties comparable to single crystal material.

Placing our results in their proper context, we choose to emphasize the fact that by judicious choice of redox active electrolytes we have stabilized photoelectrodes to photoanodic dissolution. The measured conversion efficiencies are encouraging, but we note that the estimated solar energy conversion efficiency is ~1% for a SrTiO₃ based cell to photoelectrolyze H₂O to *storable fuels*.³² Despite the fact that CdSe should respond to ~50% of the sun's output and SrTiO₃ only responds to ~3%, our estimated efficiency for CdSe based cells to produce electricity from sunlight is only twice as much as for SrTiO₃ producing *storable fuels*. However, attempts to sensitize the metal oxide based cells to visible light have not met with much success thus far.

Seemingly, efficient, practical conversion of optical energy to electrical and chemical energy using photoelectrochemical cells will depend on the chemists' ability to selectively manipulate the rates of electrode reactions. The studies reported herein show convincingly that it is possible to find redox systems which will react fast enough to prevent the competitive photoanodic dissolution.⁵⁸

Experimental Section

Materials. CdS and CdSe single crystals were obtained from Cleveland Crystals, Inc. Samples were purchased as 10 × 10 × 1 mm plates with the 10 × 10 surface oriented perpendicular to the *c* axis. Resistivities, as measured by Cleveland Crystals using the four point probe method, were 2–6 Ω cm for CdS samples and ranged from 0.1 to 14 Ω cm for CdSe samples.

Electrolytes. Since sulfide and polysulfide solutions are air sensitive, all preparations and experiments were done with an Ar purge. We have found that the addition of appropriate quantities of NaOH and Na₂S·9H₂O (Mallinckrodt) to Ar purged distilled water results in stable sulfide solutions. Polysulfide solutions are prepared from purged sulfide solutions by the addition of sublimed sulfur (Baker).

Preparation of Crystals. Crystals were routinely cut to 5 × 5 × 1 mm and then etched before use as electrodes. CdS was etched in concentrated HCl for 1 min to identify the 0001 "Cd" (pitted) and 000 $\bar{1}$ "S" (matte) faces.⁵⁵ CdSe was immersed in a mixture of HNO₃, H₂SO₄, HOAc, and HCl (30:20:10:0.1 by vol.) at 50 °C for 8 s and then rinsed, first with concentrated H₂SO₄ and then water, to identify the 0001 "Cd" (specular) and 000 $\bar{1}$ "Se" (matte) faces.⁵⁶ One sample each of CdS and CdSe was polished to an optical finish with 0.1 μ alumina, and their absorption spectra were recorded on a Cary 17 spectrophotometer.

Preparation of Electrodes. Electrodes were fashioned by rubbing gallium–indium eutectic on one face of the etched crystal and attaching this to a glass-encased copper wire whose end had been coated

with silver epoxy. All exposed metal was then insulated with ordinary epoxy.

Typical Cell. Experiments were performed in a Pyrex vessel, 3 cm in diameter and 9 cm long, whose base was equipped with a stopcock so that electrolytes could be changed without disturbing the other elements of the cell. The cathode was a piece of Pt gauze 10 × 2 cm. Stirring was accomplished by bubbling Ar vigorously through the solution. Geometrical arrangement of the components of the cell was to place the photoanode as close to the wall of the vessel as possible and the Pt gauze at the opposite end. When an SCE was employed, the standard three electrode geometry was used.

Several light sources were used. Monochromatic irradiation was obtained at 632.8 nm from a Spectra Physics He-Ne laser, at 514.5, 501.7, and 454.5 nm from a Spectra Physics argon ion laser, and at 610 nm from a tunable dye laser. Intensity variation of these lines was achieved with colored filters and/or laser power. Very intense broad band visible light was provided by a Bausch & Lomb 200SP source equipped with an Osram HBO 200 W super high pressure Hg arc lamp. Excessive heat was dissipated by passing the beam through 18 cm of H₂O. A Corning 3-73 filter was used to screen the photoelectrode from irradiation of wavelengths shorter than 420 nm. Monochromatic irradiation at various wavelengths throughout the visible and near ir was isolated by passing the output of a 600 W GE tungsten halogen lamp through a Bausch & Lomb high intensity monochromator. Light intensity was measured with a Tektronix J16 digital photometer equipped with a J6502 probe.

Current-Voltage Curves. Two kinds of curves were obtained: (1) Photocurrent as a function of applied potential from a HP 6241 power supply in series in the external circuit; for these curves the current was measured by monitoring the potential drop across a 100 Ω resistor in series in the circuit. (2) A standard three electrode cell was used to obtain curves where the photoanode is potentiostated against an SCE. Potentiostating was accomplished with a Heath EUA-19-2 Polarography Module.

Wavelength Dependence. Relative photocurrent as a function of excitation wavelength was determined by using monochromatized light from the tungsten halogen lamp. The lamp's intensity as a function of wavelength from 450 to 800 nm was measured with the Tektronix photometer. Photocurrents were then obtained (see circuit 1 of current-voltage curves) at zero bias in 1.0 M NaOH and 1.0 M Na₂S as a function of wavelength and corrected for the variation in light intensity. A second curve was obtained in a like manner by using an Aminco Bowman SPF-2 emission spectrometer with a 150 W xenon excitation lamp and correcting for variation in lamp intensity as a function of wavelength (400–600 nm) using a Rhodamine B quantum counter.⁵⁷

Quantum Yields. Quantum yields for electron flow were measured in both sulfide and polysulfide electrolytes. Beam-expanded lasers with output at 632.8, 610, 514.5, 501.7, and 454.5 nm served as light sources. The beam was masked to just fill the crystal surface, and photocurrent as a function of applied potential (see circuit 1 of current-voltage curves) was determined. Light intensity was then measured with the Tektronix photometer described above.

Open-Circuit Photopotential. A high impedance HP 7101B strip chart recorder in series with the photoelectrode and Pt gauze was used to measure the open-circuit photopotential. Beam-expanded laser lines at 501.7 and 514.5 nm were masked to just fill the photoelectrode surface. A beam splitter was employed in conjunction with the Tektronix photometer to monitor intensity at the photoelectrode.

Stability. Visible-uv spectra required to monitor electrolyte stability during electrolyses were taken with the Cary 17. The conventional electrolysis of polysulfide was run in 0.1 mm path length cells obtained from Precision Cells, Inc. Electrode stability tests were made under a variety of conditions. After long-term irradiation the crystal was demounted by dissolving the epoxy in CH₂Cl₂. Weight changes were determined to ±0.1 mg.

Current-Voltage Curves as a Function of Wavelength. The monochromatized output of a 600 W tungsten halogen lamp was determined at several wavelengths with the Tektronix photometer. Monochromator slits were adjusted to make the intensities at these wavelengths equivalent in terms of einsteins/second. Potentiostated curves were then taken with the three electrode cell described earlier as a function of the intensity-adjusted wavelengths.

Acknowledgment. We thank the National Aeronautics and Space Administration for support of this work. We acknowl-

edge the assistance of Peter T. Wolczanski, and we thank Professor R. Field for access to his tunable dye laser for studies of CdSe based cells at 610 nm.

References and Notes

- (1) Fannie and John Hertz Foundation Fellow.
- (2) Fellow of the Alfred P. Sloan Foundation, 1972–1974, and a Dreyfus Teacher-Scholar Grant recipient, 1975–1980.
- (3) A. B. Ellis, S. W. Kaiser, and M. S. Wrighton, *J. Am. Chem. Soc.*, **98**, 1635 (1976).
- (4) K. Bohenkamp and H. J. Engell, *Z. Elektrochem.*, **61**, 1184 (1957).
- (5) U. R. Harten, *Z. Naturforsch., A*, **16**, 1401 (1961).
- (6) R. Williams, *J. Chem. Phys.*, **32**, 1505 (1960).
- (7) R. A. L. Vanden Berghe, W. P. Gomes, and F. Cardon, *Z. Phys. Chem. (Frankfurt am Main)*, **92**, 91 (1974).
- (8) V. A. Tyagai and G. Ya. Kolbasov, *Surf. Sci.*, **28**, 423 (1971).
- (9) A. Fujishima, E. Sugiyama, and K. Honda, *Bull. Chem. Soc. Jpn.*, **44**, 304 (1971).
- (10) F. Sitabkhan, *Ber. Bunsenges. Phys. Chem.*, **76**, 383 (1972).
- (11) Cf. the points raised by G. C. Barker in the Discussion following the paper: H. Gerischer, *J. Electrochem. Soc.*, **113**, 1174 (1966).
- (12) H. Gerischer and W. Mindt, *Electrochim. Acta*, **13**, 1239 (1968).
- (13) E. Becquerel, *C. R. Hebd. Seances Acad. Sci.*, **9**, 561 (1839).
- (14) Yu. V. Pleskov and Z. A. Rotenberg, *J. Electroanal. Chem.*, **20**, 1 (1969), and references therein.
- (15) (a) H. Gerischer, "Physical Chemistry: An Advanced Treatise", Vol. 9A, H. Eyring, D. Henderson, and W. Jost, Ed., Academic Press, New York, N.Y., 1970, Chapter 5; (b) H. Gerischer, *Adv. Electrochem. Electrochem. Eng.*, **1**, 139 (1961); (c) V. A. Myamlin and Yu. V. Pleskov, "Electrochemistry of Semiconductors", Plenum Press, New York, N.Y., 1967; (d) T. Freund and W. P. Gomes, *Catal. Rev.*, **3**, 1 (1969).
- (16) H. Gerischer, *J. Electroanal. Chem.*, **58**, 263 (1975).
- (17) R. C. Young, T. J. Meyer, and D. G. Whitten, *J. Am. Chem. Soc.*, **97**, 4781 (1975), and references therein.
- (18) W. M. Latimer, "Oxidation Potentials", 2d ed, Prentice Hall, New York, N.Y., 1952, p. 42.
- (19) A. Fujishima and K. Honda, *Nature (London)*, **238**, 37 (1972); *Bull. Chem. Soc. Jpn.*, **44**, 1148 (1971).
- (20) M. S. Wrighton, D. S. Ginley, P. T. Wolczanski, A. B. Ellis, D. L. Morse, and A. Linz, *Proc. Natl. Acad. Sci. U.S.A.*, **72**, 1518 (1975).
- (21) J. Keeney, D. H. Weinstein, and G. M. Haas, *Nature (London)*, **253**, 719 (1975).
- (22) (a) S. N. Frank and A. J. Bard, *J. Am. Chem. Soc.*, **97**, 7427 (1975); (b) K. L. Hardee and A. J. Bard, *J. Electrochem. Soc.*, **122**, 739 (1975).
- (23) A. J. Nozik, *Nature (London)*, **257**, 383 (1975).
- (24) T. Ohnishi, Y. Nakato, and H. Tsubomura, *Ber. Bunsenges. Phys. Chem.*, **79**, 523 (1975).
- (25) J. H. Carey and B. G. Oliver, *Nature (London)*, **259**, 554 (1976).
- (26) H. Yoneyama, H. Sakamoto, and H. Tamura, *Electrochim. Acta*, **20**, 341 (1975).
- (27) A. Fujishima, K. Kohayakawa, and K. Honda, *Bull. Chem. Soc. Jpn.*, **48**, 1041 (1975); *J. Electrochem. Soc.*, **122**, 1437 (1975).
- (28) J. G. Mavroides, D. I. Tchernev, J. A. Kafalas, and D. F. Kolesar, *Mater. Res. Bull.*, **10**, 1023 (1975).
- (29) W. Gissler, P. L. Lensi, and S. Pizzini, *J. Appl. Electrochem.*, **6**, 9 (1976).
- (30) L. A. Harris and R. H. Wilson, *J. Electrochem. Soc.*, **123**, 1010 (1976).
- (31) M. S. Wrighton, D. L. Morse, A. B. Ellis, D. S. Ginley, and H. B. Abrahamson, *J. Am. Chem. Soc.*, **98**, 44 (1976).
- (32) M. S. Wrighton, A. B. Ellis, P. T. Wolczanski, D. L. Morse, H. B. Abrahamson, and D. S. Ginley, *J. Am. Chem. Soc.*, **98**, 2774 (1976).
- (33) J. G. Mavroides, J. A. Kafalas, and D. F. Kolesar, *Appl. Phys. Lett.*, **28**, 241 (1976).
- (34) A. B. Ellis, S. W. Kaiser, and M. S. Wrighton, *J. Phys. Chem.*, **80**, 1325 (1976).
- (35) D. C. Cronemeyer, *Phys. Rev.*, **87**, 876 (1952).
- (36) M. Nagasawa and S. Shionoya, *J. Phys. Soc. Jpn.*, **30**, 1118 (1971).
- (37) (a) T. A. Noland, *Phys. Rev.*, **94**, 724 (1954); (b) M. Cardona, *ibid.*, **140**, A651 (1965); (c) M. I. Cohen and R. F. Blunt, *ibid.*, **168**, 929 (1968).
- (38) D. Khang and S. H. Wemple, *J. Appl. Phys.*, **36**, 2925 (1965).
- (39) M. DiDomenico, Jr., and S. H. Wemple, *Phys. Rev.*, **166**, 565 (1968).
- (40) A. K. Ghosh and H. P. Maruska, Abstract No. 220, 149th Meeting of The Electrochemical Society, Washington, D.C., 1976, and to be published in the Proceedings entitled, "International Symposium on Solar Energy".
- (41) (a) H. Gerischer and H. Tributsch, *Ber. Bunsenges. Phys. Chem.*, **72**, 437 (1968); **73**, 251 (1969); (b) H. Gerischer, M. E. Michel-Beyerle, F. Rebenstrost, and H. Tributsch, *Electrochim. Acta*, **13**, 1509 (1968).
- (42) H. Gerischer, *Photochem. Photobiol.*, **16**, 243 (1972); *Ber. Bunsenges. Phys. Chem.*, **77**, 771 (1973).
- (43) Y. Nakato, T. Ohnishi, and H. Tsubomura, *Chem. Lett.*, 883 (1975).
- (44) J. O'M. Bockris and K. Uosaki, Abstract No. 14, Inorganic Division, 100th National Meeting of the American Chemical Society, New York, N.Y., 1976, and *Adv. Chem.*, to be published.
- (45) Y. G. Chai and W. W. Anderson, *Appl. Phys. Lett.*, **27**, 183 (1975).
- (46) H. Gerischer and H. Rösler, *Chem.-Ing.-Tech.*, **42**, 176 (1970).
- (47) H. Gerischer, *J. Electrochem. Soc.*, **113**, 1174 (1966).
- (48) R. A. L. Vanden Berghe, W. P. Gomes, and F. Cardon, *Ber. Bunsenges. Phys. Chem.*, **77**, 289 (1973).
- (49) The exact composition of the electrolyte used in ref 16 was not given, but presumably it was aqueous KCl.
- (50) (a) D. Dutton, *Phys. Rev.*, **112**, 785 (1958); (b) R. G. Wheeler and J. Dimmock, *ibid.*, **125**, 1805 (1962).
- (51) At least for low applied potentials and small current densities, polysulfides

- can be reversibly oxidized and reduced: P. L. Allen and A. Hickling, *Trans. Faraday Soc.*, **53**, 1626 (1957), and references therein.
- (52) W. Giggenbach, *Inorg. Chem.*, **11**, 1201 (1972), and references therein.
- (53) For distribution of terrestrial solar insolation, cf. M. D. Archer, *J. Appl. Electrochem.*, **5**, 17 (1975).
- (54) H. Kim and H. A. Laitinen, *J. Electrochem. Soc.*, **122**, 53 (1975).
- (55) D. C. Reynold and L. C. Green, *J. Appl. Phys.*, **29**, 59 (1958).

- (56) E. P. Warekols, M. C. Lavine, A. N. Mariano, and H. C. Gatos, *J. Appl. Phys.*, **33**, 690 (1962).
- (57) W. H. Melhus, *J. Opt. Soc. Am.*, **52**, 1256 (1962).
- (58) NOTE ADDED IN PROOF. We wish to call attention to the related work which has recently appeared in communication form: G. Hodes, J. Manassen, and D. Cahen, *Nature (London)*, **261**, 403 (1976), and B. Miller and A. Heller, *ibid.*, **262**, 680 (1976).

Electrochemical Studies on Sulfur and Sulfides in AlCl₃-NaCl Melts

Knut A. Paulsen and Robert A. Osteryoung*

Contribution from the Department of Chemistry, Colorado State University, Fort Collins, Colorado 80523. Received February 17, 1976

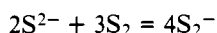
Abstract: Liquid sulfur has been reduced coulometrically in AlCl₃-NaCl melts at 175 °C. The reduction is a two-electron process yielding S²⁻. The current efficiency for the process is 100%. Copper and silver electrodes have been used for coulometric titrations of the sulfide content of the melt. By following the potential of the metal/metal ion during these titrations, the solubility product of cuprous and silver sulfide in the basic melt at 175 °C has been determined. The solubility of metal sulfides was found to increase markedly as the melt was made more acid, i.e., as AlCl₃ was added. Nernst plots for the sulfur-sulfide redox couple have a slope corresponding to a four-electron reaction, which may be represented as S₂ + 4e⁻ = 2S²⁻. From the variation of the S₂/S²⁻ redox potential with melt acidity, it is deduced that the acid-base equilibrium involving sulfide and the solvent may be AlCl₄⁻ + S²⁻ = AlSCl + 3Cl⁻. The oxidation of sulfur yields cations of oxidation state +1 or higher.

Electrochemical studies of sulfur and sulfides in molten salts have received considerable attention in recent years.^{1-9,14,16-19}

Delarue^{1,2} investigated redox reactions involving sulfur and sulfides in lithium chloride-potassium chloride melts. He quantitatively studied the solubility of a series of sulfides in the eutectic melt. The sulfides of manganese(II), thallium(I), and of the alkaline and earth alkaline metals were soluble, whereas sulfides of Zn²⁺, Cd²⁺, Ni²⁺, Co²⁺, Ag⁺, Sn²⁺, Sb³⁺, Bi³⁺, Pd²⁺, Pt²⁺, Cu⁺, Fe²⁺, Ce³⁺, and Pb²⁺ were insoluble. Sulfides of copper(II), iron(III), gold(I) and mercury(II) reacted in the melt; the metal ions were reduced and sulfide oxidized to sulfur.

Bodewig and Plambeck^{3,4} studied sulfur-sulfide solutions in LiCl-KCl eutectic by potentiometric, voltammetric, chronopotentiometric, and spectrophotometric techniques. The sulfur-sulfide couple showed Nernstian behavior with a value of 1.86 for the number of electrons taking part in the reaction. Their Nernst plots were made by coulometrically reducing sulfur from a saturated solution, thus maintaining the sulfur activity constant. Coulometric titrations of anodically generated Fe²⁺, Ni²⁺, Co²⁺, and Ag⁺ by reduction of a sulfur pool electrode produced potentiometric titration curves with breaks of 160-400 mV. These breaks were reported to occur a considerable, but not a reproducible, distance before the theoretical equivalence point. Solutions containing both sulfur and sulfide had a blue color. Since it disappeared when either sulfur or sulfide was absent, they postulated that the color was due to a polysulfide ion formed by sulfur and sulfide; i.e., S²⁻ + xS ⇌ S_{x+1}²⁻.

Gruen et al.⁵ carried out spectrophotometric measurements on the sulfur-sulfide system in LiCl-KCl. The spectrum of dissolved sulfur had its maximum at 36 000 cm⁻¹, close to the absorption peak of gaseous S₂ molecules. On the basis of the absorption spectra for sulfur-sulfide solutions, they propose the two equilibria between sulfur and sulfide:



The S₃⁻ ion is attributed to the ultramarine blue color and the S₂⁻ ion to ultramarine green.

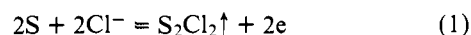
Giggenbach¹⁸ concluded from his spectrophotometric measurements in LiCl-KCl that S₂⁻ is responsible for the blue color. The blue melt loses its color on cooling to temperatures below 400 °C, which is ascribed to the dimerization of S₂⁻ ions to form S₄²⁻ ions.

Bernard et al.¹⁹ carried out chronopotentiometric and spectrophotometric measurements on sulfide in LiCl-KCl eutectic. Calcium sulfide was dissolved in the melt and the sulfide was said to be oxidized in three steps. The ultimate products of oxidation and reduction were said to be S⁺ and S²⁻, respectively. The three sulfide species S²⁻, S_x²⁻, and S_y⁻ were attributed to absorption bands at 320, 390, and 590 nm. The most probable values for y were 2 or 3 and for x, 5.

Cleaver et al.¹⁷ found that Na₂S was practically insoluble in the LiCl/KCl eutectic at 420 °C and no cyclic voltammetric waves could be observed. Addition of Na₂S_{2.2} gave lime green solutions which lost sulfur gradually. Cyclic voltammograms using a gold electrode showed two redox couples. The waves at the most negative potentials were attributed to a one-electron process: S₂²⁻ → S₂⁻ + e. The other waves were deposition and stripping of sulfur. Sulfur was found to be the final oxidation product.

Liu et al.⁶ determined the solubility product for NiS and Li₂S in the LiCl/KCl eutectic. They developed a NiS/Ni electrode which gave very large potential breaks at the end point when sulfide was titrated with coulometrically generated Ni(II).

King and Welch¹⁶ studied electrolysis of metal sulfide in chloride melts. They showed that, for production of lead, dissolution of sulfur was the major contributor to the lowering of cathodic current efficiency. When the limiting current density for sulfur evolution was reached, the anode potential increased rapidly to that of the next process, evolution of sulfur monochloride,



Two papers deal with the behavior of sulfur in a low-tem-